Summer monsoon belt displacement and precipitation sources in the Northern Arabian Sea: A multi-proxy palaeoenvironmental reconstruction for Late Holocene

Sedigheh Amjadi, Mohammad H M Gharaie, Hamid H K Lahijani, David Kaniewski, Razieh Lak, Majid Pourkerman, Majid Shah-Hosseini, Mohammad- Ali Hamzeh, Nick Marriner

Caspian Journal of Environmental Sciences
Online ISSN: 1735-3866
Print ISSN: 1735-3033

Summer monsoon belt displacement and precipitation sources in the Northern Arabian Sea: A multi-proxy palaeoenvironmental reconstruction for Late Holocene

Sedigheh Amjadi[1], Mohammad H.M. Gharaie*[1], Hamid H.K Lahijani[2], David Kaniewski[3], Razieh Lak[4], Majid Pourkerman[4], Majid Shah-Hosseini[5], Mohammad-Ali Hamzeh[2], Nick Marriner[6]

1. Department of Geology, Faculty of Science, Ferdowsi University of Mashhad, Mashhad, Iran
2. Iranian National Institute for Oceanography and Atmospheric Science (INIOAS), Tehran, Iran
3. TRACES, UMR 5608 CNRS, Université Toulouse Jean Jaurès, Maison de la Recherche, 5 Allées A. Machado, 31058, Toulouse, Cedex 9, France
4. Research Institute for Earth Sciences, Geological Survey of Iran, Tehran, Iran
5. Department of Geography, Tarbiat Modares University, P.O. Box 14115-175, Tehran, Iran
6. CNRS, ThéMA, Université de Franche-Comté, UMR 6049, MSHE Ledoux, 32 Rue Mégevand, 25030, Besançon, Cedex, France

** Corresponding author's Email: mhmgharaie@um.ac.ir*

ABSTRACT

The identification of precipitation sources and palaeoenvironmental changes in the Arabian Sea during the late Holocene could improve our knowledge of future variations in the summer monsoon. In this study, we compare and contrast foraminifera, stalagmite isotopes, clay mineralogy and palaeooceanographic data in order to shed new light on the interactions between atmospheric and oceanographic parameters on the summer monsoon belt displacement and precipitation sources during the late Holocene. We showed that during warm periods (e.g. the Roman and Medieval periods), the increased intensity of northern Levar winds led to a decrease in summer monsoon precipitation in the northern Arabian Sea. Increased wind stress from the north led to the transportation of warm and saline water from the Persian Gulf to the northeast of the Arabian Sea. These conditions were favorable to the regeneration of tropical storms originating in the Bay of Bengal, between 1900 and 1500 calyr BP (similar to Golab-Shaheen tropical cyclone). By contrast, maximum summer monsoon winds are observed during cooler periods when N Levar winds were weakest. A poleward movement of the summer monsoon belt that happened around 1400 calyr BP led to an increase in NW summer Shamal wind intensity, increased Persian Gulf outflow to the Gulf of Oman, cold-water upwelling events in the eastern part of the Oman Gulf and increases in water temperature in the center of the Arabian Sea. Consequently, the number of tropical storms originating in the Arabian Sea (e.g. similar to Gonu and Phet) increased during cooler periods. These data provide a template to understand the present and future evolution of the summer monsoon in the Arabian Sea, under climate change.

Keywords: Monsoon, Tropical storm, Late Holocene, Gulf of Oman, Arabian Sea.
Article type: Research Article.

INTRODUCTION

The summer monsoon occurs from June to September. The summer monsoon precipitation affects many countries, such as China, Bangladesh, Japan, and etc., however, it is vital for the ecosystems and agricultural systems of northern India, which hosts 7% of the world's population (Yadav & Roxy 2019). Therefore, spatio-temporal changes in the summer monsoon could have potentially serious impacts on water availability and drought in South Asia. Monsoon variability is closely linked with northern hemisphere temperatures and aerosols (Sinha et al.

2015). During the Roman Climatic Optimum (2300 to 1900 calyr BP), concurrent with the domination of arid climatic conditions over the Sistan Basin, the intensity of summer monsoon precipitation decreased under the influence of dust storm events (Amjadi 2023). By the second half of the twentieth century, anthropogenic aerosols had significantly impacted monsoon precipitation in comparison with greenhouse gases or natural forcing agents (Polson *et al.* 2014). Hydrological cycle changes linked to anthropogenic activities can have serious impacts on climate change and create aerosol sources (Ginoux *et al.* 2012; Golobokova *et al.* 2020; Ahmad *et al.* 2022). Dust storms and transportation of aerosols to the Arabian Sea are influenced by two important wind regimes (Fig. 1). The poleward movement of the summer monsoon belt creates strong wind over continental Arabia (summer Shamal wind; Alizadeh-Choobari *et al.* 2014). The summer Shamal wind is an intensive northwest one that is generated due to the pressure gradient between the high pressure system over the eastern Mediterranean and the summer monsoon low pressure over the Arabian Sea. The Shamal wind blows between mid-May to mid-August over the Arabian Peninsula and SW Asia (Hamidi *et al.* 2014). It can attain speeds of more than 100 km h^{-1} (Garzanti *et al.* 2013) and its intensity increases during La Niña (Yu *et al.* 2015). The Shamal wind transports huge quantities of dust aerosols to the Arabian Sea, mobilized when it blows through Mesopotamia, the eastern Arabian Peninsula and the Persian Gulf (Al Senafi & Anis 2015; Maghrabi & Al-Dosari 2016; Hamidi *et al.* 2017). The most important clay mineral that is entrained and transported by the Shamal wind is palygorskite from southern Mesopotamia (Aqrawi 1993; Hassanizade & Jafari 2021). The pressure gradient difference between the Caspian Sea and the Hindu Kush mountains generates strong north Levar winds (>72 km h^{-1}) that occur between June and September (Alizadeh-Choobari et al. 2014). Dust storm events under the influence of the Levar wind transport huge amounts of aerosols from the Karakum desert in Turkmenistan, Jazmurian and Hamun ephemeral lake in the Sistan Basin (Kaskaoutis *et al.* 2015; Fig. 1). The intensity of the Levar wind increases concurrently by an intensification of the pressure gradient between the Caspian Sea and the Hindu Kush mountains during the poleward migration of the summer monsoon belt (Rashki *et al.* 2019). Dust storms have a significant impact on the Northern coast of the Arabian Sea, Gulf of Oman, western Pakistan, and the southeastern Arabian Peninsula (Rashki *et al.* 2017). The other source of the aerosol in the Arabian Sea is from the NE of Africa, characterized by palygorskite as the main clay mineral. Clay minerals are widely used for identifying sediment sources and reconstructing paleoclimatic and paleoenvironmental conditions (Alizai *et al.* 2012; Clift *et al.* 2014). Aerosol analysis in the Arabian Sea revealed different sources of clay minerals. Northern Africa is characterized by smectite and palygorskite, which are derived from arid and semi-arid regions. The Arabian Peninsula is characterized by high illite and palygorskite, which are associated with dust storms and soil erosion. The SW Asia, Indus Plains, and the Thar Desert are rich in illite and chlorite, which are influenced by the Himalayan orogeny and glacial activity. Finally, the Indian Peninsula has high smectite and chlorite due to the weathering of Deccan Trap basalts. Seasonal variability in aeolian deposition in the Northeastern Arabian Sea shows that during dry periods illite and chlorite are dominant clay minerals, while during wet periods smectite and palygorskite become more prevalent (Suresh *et al.* 2022). Dust aerosol imports into the Arabian Sea significantly increase marine nutrients and biological productivity (Liao *et al.* 2016). Primary productivity in the Arabian Sea is mainly controlled by iron from aerosol imports and cold-water upwelling (Al-Azri *et al.* 2010; Guieu *et al.* 2019). Therefore, foraminifera are good markers to evaluate both environmental and palaeoceanographic changes (Munz *et al.* 2015; Ladigbolu *et al.* 2020; Saravanan *et al.* 2020). Foraminifera abundance is not only dependent on nutrient availability but is also controlled by other physical and chemical factors such as dissolved oxygen, salinity, water stratification and turbidity. The Gulf of Oman lies within the northern edge of inter-tropical convergence zone (ITCZ) and is located in the zone of climatic change between the Mediterranean depressionary systems (Meher-Homji 1991; Modarres & Rodrigues 2007). The climate in the Gulf of Oman is controlled seasonally by Indian monsoon precipitation. Salinity in the Gulf of Oman is mediated by the depth of the Persian Gulf's outflow and oceanographic currents. During the summer monsoon, cold-water upwelling in the off eastern coast of Oman part of Gulf of Oman leads to a decrease in the depth of the Persian Gulf warm and saline outflow into the Gulf of Oman (Pourkerman *et al.* 2023). As a result of the increase in upwelling intensity, the summer monsoon wind stress can generate a major biogeographic barrier in the Northern Arabian Sea (Reuter *et al*. 2022) and the Gulf of Oman. Although palaeo-environmental reconstructions employing biological indicators such as dinoflagellate cysts and foraminifera have been widely used for environmental reconstructions (Li *et al.* 2021; Azharuddin *et al.* 2022), oceanographic currents can create considerable bias in palaeoclimatological interpretations. To this end, there are significant knowledge gaps that remain with regards to the impacts of

changes in summer monsoon wind stress in the northern part of the Arabian Sea. The aim of this study is to employ clay mineralogical analysis in order to identify the main wind regimes in the Arabian Sea and their impacts on summer monsoon variation during the late Holocene.

MATERIALS AND METHODS

Core OM15 (locating 60.062 ºE and 25.134 ºN; Length: 166 cm) was retrieved at a water depth of 310 m in western part of the Makran continental margin, ~30 km off the Iranian coast (Fig. 1). The core was taken in 2012 using a gravity corer during the Persian Gulf and Gulf of Oman cruise Magnetic Susceptibility (MS) was measured at a 2-cm resolution using a Bartington MS2C 100-mm diameter loop sensor. High-resolution sampling was conducted on the studied core and 80 samples were collected following the sampling procedure described by Marriner & Morhange (2007). Each sample was divided into two sub-samples to measure organic matter (OM), carbonate content and grain size. Wet sieving was used to separate the >2 mm and <63 µm fractions. OM and carbonate content were measured using Loss-On-Ignition (LOI) at 550 °C and 950 °C (Heiri *et al.* 2001).

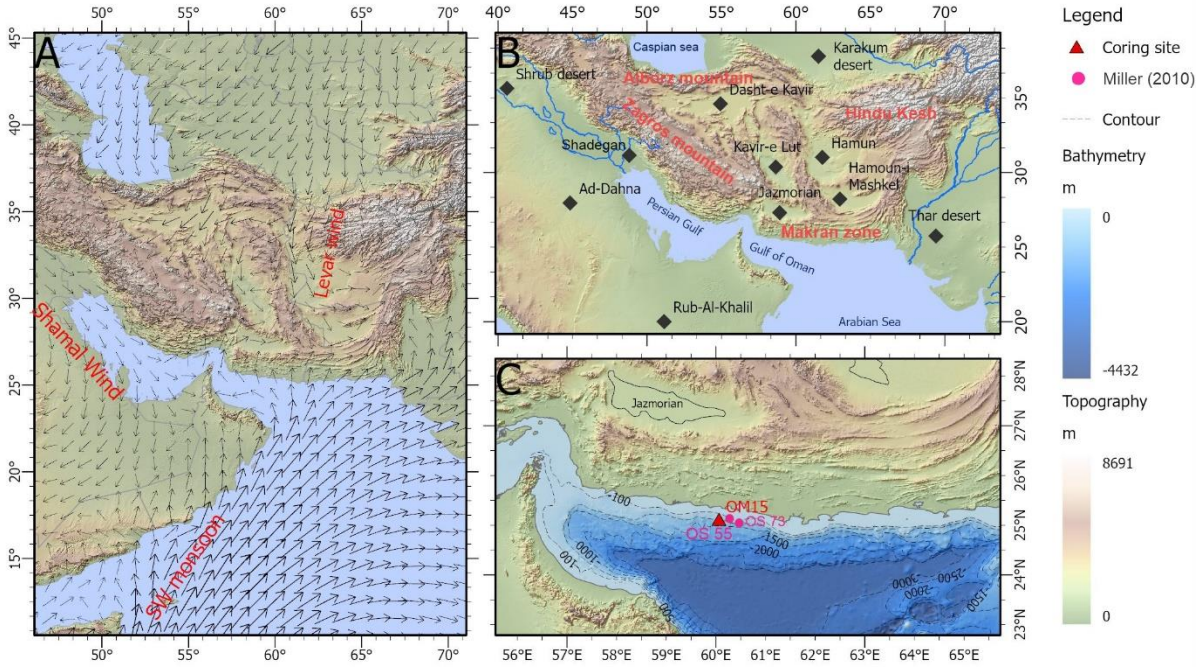

Fig. 1. General direction of Levar and summer monsoon and Shamal winds. The wind derives from the global ocean surface wind stress database (https://doi.org/10.48670/moi-00305) for severe dust storms during 3-8 July 2009 (Hamidi *et al*. 2014). B) Location of major dust sources in the Middle East and C) location of core site in the northern part of the Gulf of Oman, the purple cycles are location of studied cores by Miller (2010).

The chronology is based on an age-depth model using calibrated 210Pb and radiocarbon dating for two cores (OS55 and OS73) from the Gulf of Oman, studied by Miller (2010). According to the 210Pb, first 20 cm of core OS55 had an average sedimentation rate of 2.3 mm yr^{-1}. Core OS73 had a settling rate of 0.7-2.42 mm yr^{-1}, based on three calibrated radiocarbon ages at 65, 120.5, and 148.5 cm (Miller 2010). The study core was at the same location as two cores studied by Miller (2010) in terms of bathymetry and distance from the shoreline (Fig. 1). In order to use the data for the current study, it is necessary to compare the sedimentation rate and environmental condition between these cores. To address this issue, we used magnetic susceptibility (MS) data from core OM15 and OS73. MS of the ocean sediment is strongly controlled by the bottom current condition (Moros *et al.* 2002). The MS correlation could be overprinted by changes in the sediment source and the presence of highly magnetic material or dilution with non-magnetic material (Pirrung *et al.* 2002). As a result, because of the strong relationship with environmental condition, MS of deep sea is widely used as a correlative tool at local and basin-wide scales (Thompson & Clark 1989; Robinson *et al.* 1995). Therefore, based on the chronological data, an age-depth model was created for the study cores. The clay minerals were identified by X-ray diffraction (XRD) using a Philips PW1800 instrument in Kan-Pazhouh Co, Iran. The XRD analysis was performed on the <2µm siliciclastic fractions. The samples were separated by centrifugation following Stokes's settling velocity principal after

removing organic and carbonate matter using 10% hydrogen peroxide and glacial acetic acid. The clay solutions were pipetted on to glass slides to make oriented slide. The slides were subsequently air dried. Three analysis conditions were employed in order to identify clay mineral quantification: air-dry, ethylene glycol solvation (60 ºC for 12 h) and heating (490 ºC for 2 h). All patterns were collected and the peak area measurements for specific minerals were made using the software Profex ver.5.0. The clay mineral groups were identified based on the position of the (001) series of the basal reflection of specific minerals on the three XRD diagrams. A smectite-illite composed mixed layer peak (15-17 Å) was considered for smectite group. The basal reflection of the main clay mineral groups of kaolinite/chlorite (7 Å), illite (10 Å) and smectite (15-17 Å) were calculated on the glycolated curve according to the semi-quantitative estimates of peak areas (Yu *et al.* 2017). Scanning Electron Microscope (SEM) and energy dispersive X-ray spectroscopy (EDS) analyses were employed for the clay mineralogy and morphology studies. SEM-EDS was employed for 7 bulk air-dried core subsamples using a ZEISS sigma/VP instrument at the geological survey of Iran (GSI). For the biostratigraphy, the sub-samples were oven-dried at 50 °C for 12 hours. Foraminifera were subsequently picked from the >125-µm size fractions and placed on palaeontological slides for identification and counting (Marriner *et al.* 2005). Both planktonic and benthic foraminifera species were identified (Holbourn 2013; Lei & Li 2016). We compared and contrasted the acquired results of the OM15 core with reconstructed SST for the Persian Gulf and the Arabian Sea, as well as stalagmite data from northern Iraq (as a proxy for winter precipitation) and monsoon intensity.

RESULTS

Chronological data

There is a significant correlation between the MS of cores OM15 and OS73. The correlation is observed throughout the cores except for 80-85 cm (Fig. 2). This suggests that the sedimentation rate and environmental condition in both cores are almost the same. Therefore, it allows us to create an age-depth model at centennial scale by combining Pb isotope and radiocarbon dating provided by Miller (2010).

Lithological study

Core OM15 has a homogenous muddy texture. The mud content varies between 97.5 and 99.2% Wt from the base to the top, with an interruption during 2200 to 2000 calyr BP (Fig. 3). By this time, the SEM images show needle-like carbonate grains embedded in the muddy texture (Fig. 4). By the 2100 to 2000 calyr BP, the sediment grain size increased significantly along with the carbonate content, while the organic matter (OM) and magnetic susceptibility (MS) decreased. The coarse fractions are mainly composed of shell debris that were transported by debris flows. Between 2000-1750 calyr BP, the mud content increased along with OM and MS, while, the carbonate content decreased. This time interval was marked by strong fluctuations in all the studied sedimentological parameters (Fig. 3). No significant changes were observed for granulometric parameters until 1100 calyr BP. Between 1000 and 700 calyr BP, an increasing trend of OM and MS was observed and it decreased by 650 calyr BP. Since 200 calyr BP, MS and OM have shown an increasing trend in the study core. The abundance of needle-like carbonates increased in the muddy context around 150 calyr BP.

Clay mineralogy

Clay minerals are mainly composed of kaolinite, illite, smectite, and chlorite. By the 2200-2000, abundance of kaolinite increased dramatically and reached 86.15%. Meanwhile, a decreasing trend was observed for chlorite and illite. The reduction in kaolinite coincided by elevation in abundance of chlorite, illite and smectite between 2000 and 1750 calyr BP. The clay minerals did not show significant changes until 1100 calyr BP, when a sudden rise in the abundance of chlorit was detected. Between 650 and 450 calyr BP, the increase of smectite coincided with a slight rise of kaolinite frequency. Kaolinite reached its maximum between 300 and 200 calyr BP, while illite and smectite exhibited an elevating trend. Chlorite and smectite reached their maximum between 200 and 100 calyr BP, while the abundance of kaolinite and illite dropped dramatically (Fig. 4).

Foraminifera assemblages

A total of 25761 foraminifera shells were counted in core OM15, of which 79.3% were planktonic shells. The general planktonic foraminifera assemblages were dominated by *Orbulina universa*, *Globigerina rubra*, *Globigerina bulloides* and the benthic foraminifera assemblages were controlled by *Cribrononion asiaticum*, *Uvigerina peregrine*, *Globobulimina turgida* and *Cassidulina laevigata*.

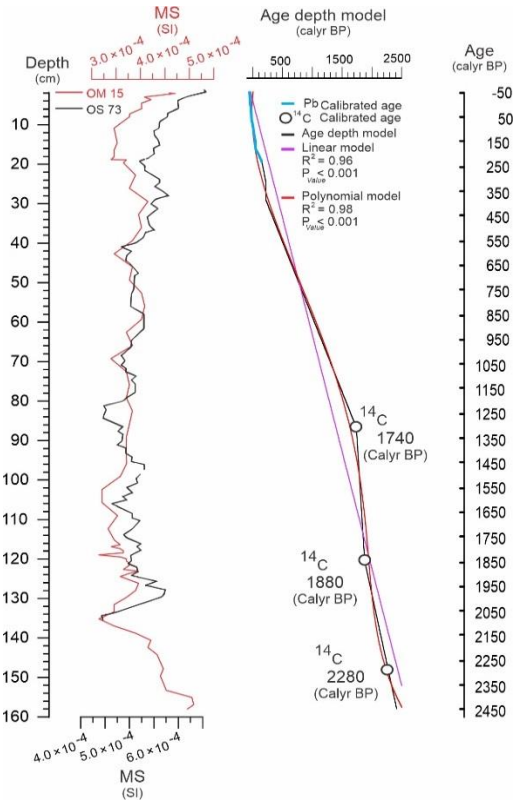

Fig. 2. Correlation between the MS of cores OM15 and OS73. The age-depth model was created according to the chronological data from Miller (2010).

Between 2100 and 2000, the most abundant planktonic species were *O. universa*, *G. bulloides* and *G. rubra* with 10199, 3473 and 3012 shells, respectively, while the dominant benthic fauna were *C. laevigata*, *C. asiaticum* and *U. peregrine* (Fig. 3). The dominance of planktonic species indicated that the nutrient availability and the dissolved oxygen level upraised due to the influx of iron-rich clay minerals and the cold water upwelling in the Gulf of Oman. These changes in environmental condition led to elevation in the foraminifera taxa and their size. Therefore, 17 foraminifera taxa were identified during this period, and most of the planktonic foraminifera size fell into the medium to coarse sand category.

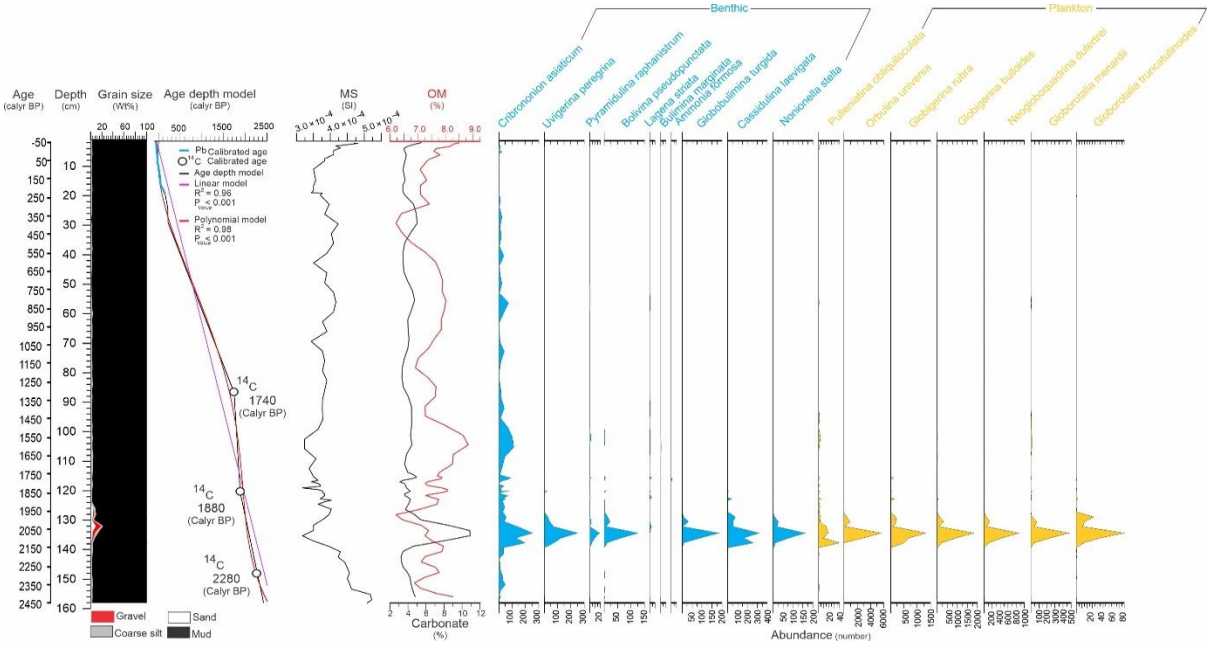

Fig. 3. Sedimentology, biostratigraphy, chronology and Magnetic Susceptibility of the core OM15.

The abundance of foraminifera taxa has dropped sharply and their sizes have rarely exceeded to over 250 micron since 2000 calyr BP. Foraminifera taxa exhibited oscillations between 2000-1750 calyr BP, especially *G. rubra*. The abundance of *G. rubra* ranged from 0 to a maximum of 147 shells, suggesting elevation in salinity by the insignificant upwelling event in the Gulf of Oman. Since 1750, *C. asiaticum* was the dominant species and its abundance decreased toward top of core. It proposed prevalence of an unsuitable environmental condition for foraminifera growth due to drop in nutrient and dissolved oxygen levels, while elevation in salinity.

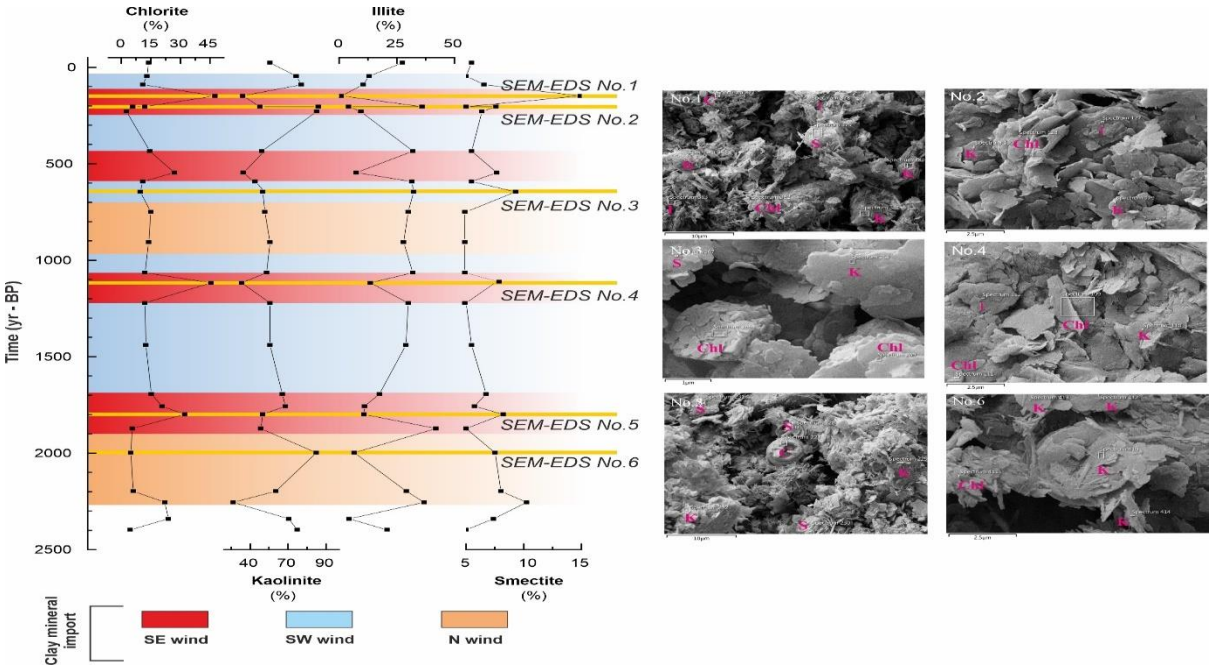

Fig. 4. Clay mineral assemblages of core OM15, with an interpretation of the dominant wind regimes. SEM image of OM15 bulk sediment from defined horizons (orange bars). The clay minerals were identified using morphology and EDS analysis points. K: Kaolinite, Chl: Chlorite; S: Smectite; I: Illite and C: carbonate.

DISCUSSION

For the late Holocene, we found that the abundance and number of foraminifera taxa have been controlled by nutrient availability and basin conditions (e.g. dissolved oxygen, salinity, temperature and turbidity; Fajemila *et al.* 2015). Sudden changes in each parameter have affected foraminifera frequency. Therefore, understanding the interaction between atmospheric and oceanographic phenomena in basin conditions are important in order to employ foraminifera and/or other biological indicators as proxies for palaeoenvironmental reconstructions. The foraminifera assemblage in the Gulf of Oman is influenced by two major factors: (i) cold-water upwelling on the eastern coast of Oman; and (ii) the volume and depth of the Persian Gulf warm and saline water outflow (Kaithwar *et al.* 2020). During the late Holocene, these variables have been controlled by the position of the summer monsoon belt and main wind regimes (NW Shamal and N Levar winds). XRD results from the study sediment core indicate the presence of kaolinite, illite, chlorite and smectite as the constituents of the clay portions. Illite and chlorite are commonly found in regions with domination of physical and mechanical weathering or in highlands where chemical weathering is minimal (Boulay *et al.* 2003). Conversely, kaolinite serves as an indicator of warm and humid tropical areas characterized by intense leaching, while smectite primarily forms through the chemical weathering of igneous rocks (Chamley 1989; Liu *et al.* 2004). Previous studies have revealed that fluvial inputs, rather than aeolian dust, are the main sources of clay minerals (illite, smectite, and chlorite) in the northeast of the Arabian Sea (Kessarkar *et al.* 2003; Thamban *et al.* 2007; Alizai *et al.* 2012; Avinash *et al.* 2016). The Indus River, as the primary source of clay constituents, annually carries 250–675 million tons of suspended sediment into the Arabian Sea, covering distances of 1000-1500 km (Rao & Rao 1995; Milliman & Farnsworth 2013). Anticlockwise water circulation through the northern Arabian Sea during the winter monsoon (Shetye *et al.* 1994; Yu *et al.* 2019) can transport clay from the Indus River along the Makran coast. A clay mineralogical study conducted on the surface sediment of Chabahar suggests that illite and chlorite account for 96% of the clay fraction (Kumar *et al.* 2020). However, the abundance of illite and chlorite in the studied core rarely exceeds 50%.

These findings indicate that clay mineralogy in the Makran coastal zone is primarily influenced by oceanographic currents rather than wind patterns. Dust inputs, on the other hand, may have a more significant impact on the clay mineral composition in the offshore zone, where the influence of longshore drift currents is negligible. The palaeoenvironmental analysis in the southeast of Iran suggests that between 2900 and 2300 calyr BP, a prolonged humid period dominated the region, coinciding with the end of the Assyrian drought and the weakening of the Siberia anticyclone (Hamzeh *et al.* 2016; Vaezi *et al.* 2022). During this humid period, intensive chemical weathering likely contributed to the generation of kaolinite. By 2400 to 2300 calyr BP, the abundance of kaolinite had reached 75%, possibly due to alluvial activities or short-term drought in the Sistan Basin and Jazmurian playa (Fig. 4). By the Roman Climatic Optimum (RCO) between 2300-1900 calyr BP, arid climatic conditions dominated in the Sistan Basin (Hamzeh *et al.* 2016). Between 2300 and 2250 calyr BP, the amount of kaolinite dropped, while the frequencies of chlorite and illite upraised, suggesting a decline in humidity and chemical weathering. The percentage of kaolinite reached 80% between 2250 and 2050 calyr BP, coinciding with the minimum occurrence of chlorite and illite (Fig. 4). The expansion of arid climatic conditions resulted in reduced fluvial activities and the transportation of clay constituents (illite and chlorite) from highlands. At the same time, the elevated wind intensities could have contributed to the suspension of clays (kaolinite) and needle-like carbonate from dried lake and playa beds. A more intense Levar wind led to the onset of dust storms (Kaskaoutis *et al.* 2015) and Fe-rich clay inputs into the Gulf of Oman. Kaolinites comprised single plates with rounded edges (Fig. 4) suggesting an authigenic source by transportation. During the RCO, the intensity of the summer monsoon would be diminished and the N Levar wind became a dominant wind in the Arabian Sea (Amjadi 2023). Northward wind regime led to the extension of a cyclonic eddy current in the Gulf of Oman (L'Hégaret *et al.* 2013) and the Persian Gulf water outflow occurred through the northern coast of Oman. Consequently, water salinity in the Northern Gulf of Oman dropped due to cold water upwelling by Ekman transport effects (Pourkerman *et al.* 2023; Fig. 7). During the RCO period, along with the intensification of the Levar wind, there was an elevation in the nutrient availability through aerosol transportation and a drop in salinity induced by oceanographic currents. These conditions created favorable circumstances for the enhanced marine productivity, as evidenced by the elevated number of foraminifera taxa in the Northern Gulf of Oman (Fig. 5). The termination of the RCO was concurrent with the onset of a humid period in the Makran zone (Miller *et al.* 2016; Forke *et al.* 2019; Normand *et al.* 2019) and the domination of tropical storms in the Bay of Bengal (Govil *et al.* 2022). During this time interval, a decreased pressure gradient between the Hindu Kush – Pamir Mountains and the Caspian Sea attenuated the N Levar wind intensity. Furthermore, clay mineral transportation from the Sistan Basin was reduced and aerosol sources were stabilized by the onset of winter precipitation (Hamzeh *et al.* 2016; Amjadi 2023). Between 1900-1700 calyr BP, the higher amounts of smectite and chlorite in the core sample may indicate that the N Levar wind would sometimes be disrupted by the SE wind due to the NW movement of tropical storms from the Bay of Bengal. The main source of smectite is from the Deccan Traps in the Eastern Arabian Sea (Milliman & Farnsworth 2013) which can be transported through aerosols or ocean currents from the northeastern region of the Arabian Sea. The Sistan Basin and the Hamun Lake might have experienced lower temperatures and low wind deposits with association periodic precipitation during the Late Antique Little Ice Age (LALIA; Hamzeh *et al.* 2016). Meanwhile, poleward shift of the summer monsoon belt led to the resumption of precipitation in Southern Oman and onset of NW summer Shamal wind (Fleitmann *et al.* 2007; Pourkerman *et al.* 2020). Dust plumes entrained by NW Shamal wind transported palygorskite from Arabian Peninsula, Mesopotamia and Southwest Iran (Sirocko *et al.* 1991). Absent fibrous palygorskite is consistent with the negligible impacts of NW Shamal winds in the Gulf of Oman at this time. The elevated frequency of illite observed in the studied sediments and Jazmurian playa (Sharifi-Yazdi *et al.* 2022) coincided with a lighter δ13C signature in the stalagmite of Kuna Ba cave and an upraise in agricultural activities in the Jiroft valley (Sinha *et al.* 2019; Vaezi *et al.* 2022; Fig. 5). This suggests an amplified influence of winter precipitation in the Southeast Iran. Accelerating NW Shamal wind intensity increases water exchange volumes between the Persian Gulf and the Gulf of Oman via the Strait of Hormuz (Pous *et al.* 2004). Concurrently, the increasing southwest (SW) wind stress over the Gulf of Oman redirects the outflow of water from the Persian Gulf along the Iranian and Pakistani coasts (L'Hégaret *et al.* 2013; Fig. 7). Additionally, cold water upwelling occurs on the eastern coast of Oman. Rising upwelling events created multiple branches for the Persian Gulf outflow water as well as elevating salinity and temperature in shallow waters (Pourkerman *et al.* 2023). As a result, Interaction between NW Shamal wind and a northward shift of the

summer monsoon belt led to an elevation in salinity in the Gulf of Oman and a drop in the number of foraminifera taxa.

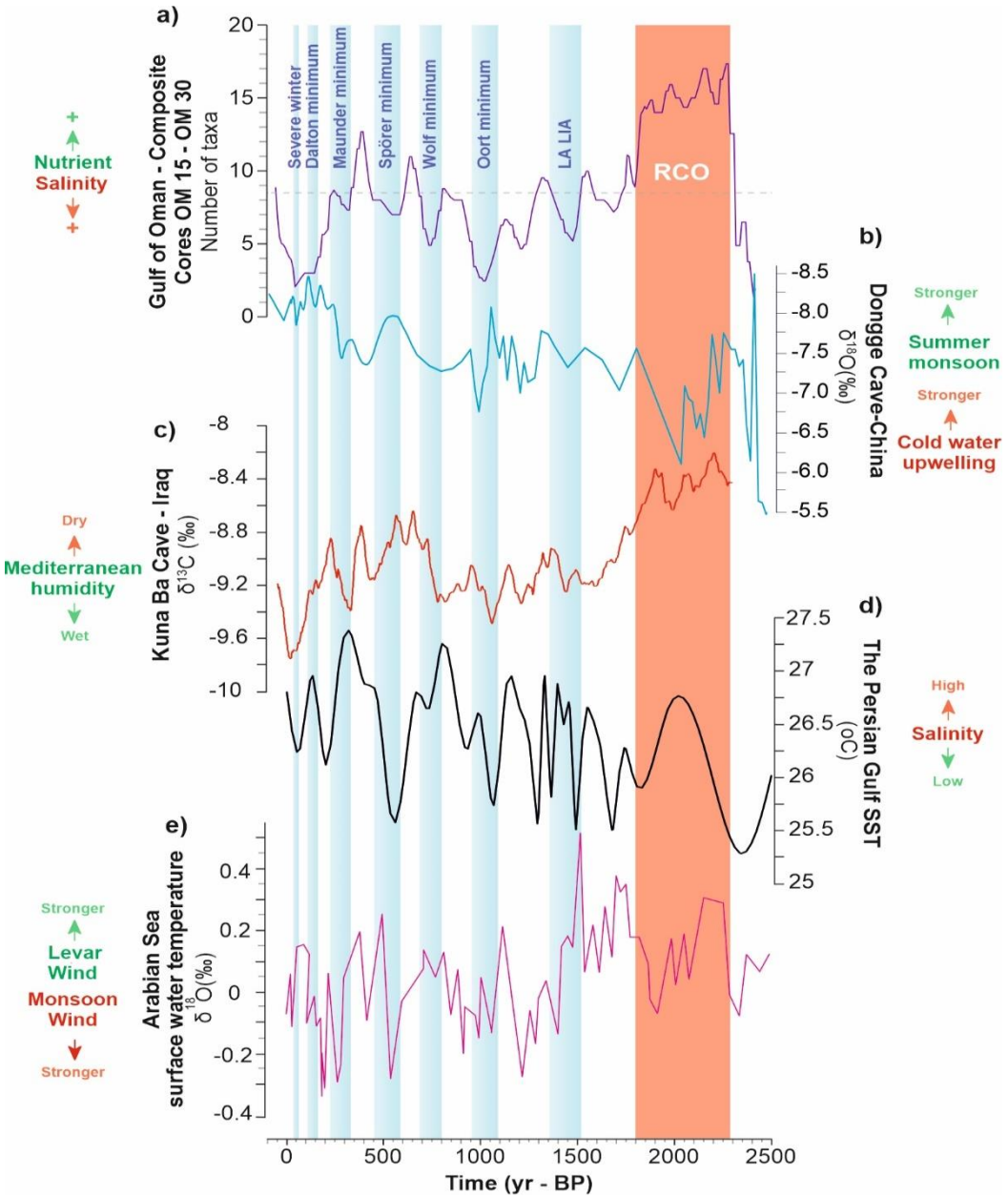

Fig. 5. a) number of foraminifera taxa in the northern Gulf of Oman sediment core (Amjadi 2023); b) Oxygen isotope record from the Dongge cave stalagmite in southeast China (Dykoski *et al.* 2005). c) Carbon isotope data from Kuna Ba cave in northern Iraq (Sinha *et al.* 2019); (d) SST changes in the eastern part of the Persian Gulf (Hamzeh *et al.* 2021); e) SST record from the northwest of the Arabian Sea (Doose-Rolinski *et al.* 2001).

The transition from Late Antiquity to the Medieval Warm Period (MWP) occurred by an elevating in SST in the Persian Gulf and the Northeast Arabian Sea (Fig. 5). The increased percentages of chlorite and smectite minerals evoke accelerating SE wind intensity following the tropical storm events around 1100 calyr BP. The record correlates with the destructive storm that struck Iran and Oman in 1085 calyr BP (Bailey 1988). Evidence of N Levar wind intensification was observed during the MWP when a dry period began in the Sistan Basin and the level of the Caspian Sea increased by ~7 to 9 meters (Krivonogov *et al.* 2014; Hamzeh *et al.* 2016). At this time, SSTs in the Persian Gulf and the Northeast Arabian Sea upraised and the foraminifera taxa record exhibited an elevating trend. The increased foraminifera taxonomic diversity in the Gulf of Oman during higher records of the Persian Gulf's SST suggests that oceanographic currents affected water outflow transportation through the northern coast of Oman during weak upwelling events. Meanwhile, domination of arid climatic conditions in the

Makran zone at this time is attested by the decreased summer monsoon precipitation (Miller *et al.* 2016). An intensification of N Levar wind created cyclonic currents in the Gulf of Oman and the dropped salinity in the northern part of the Oman Sea. The current direction was temporarily changed due to the SW monsoon wind intensification during phases of solar cycle minimum. These arid conditions continued until 300 calyr BP by an interruption during the Spörer solar cycle minimum (Fig. 5). During this cycle, SSTs in the Persian Gulf and the Northeast Arabian Sea dropped dramatically. An elevation in the abundance of smectite and chlorite suggests an acceleration in SE wind anomalies (Fig. 4). By the LIA; 300-100 calyr BP, we witness an increase in SW monsoon and summer Shamal wind intensities. Maximum impacts of the summer Shamal wind were recorded during this time by an elevation in the Persian Gulf water outflow volume and a decrease in precipitation in southern Oman. Qunf cave stalagmite $\delta^{18}O$ records from southern Oman suggest a precipitation hiatus (Fleitmann *et al.* 2007). The hiatus could be related to an eastward shift of the summer monsoon belt at the center of the Arabian Sea under the influence of strong NW summer Shamal winds. Meanwhile, summer monsoon precipitation in the Northern Arabian Sea and the Gulf of Oman is recorded by foraminifera abundance and pollen analysis. A sudden drop in foraminifera taxonomic diversity in the study core is a result of elevated upwelling events and a reduction in the Persian Gulf water outflow depth during anticyclonic current regimes in the Gulf of Oman. Meanwhile, a shift from savannah formations to Poaceae and Cyperaceae in the western Makran suggest a domination of wet climatic conditions and an increase in summer precipitation (Miller *et al.* 2016). Palynological studies in the Gulf of Oman attest to flash-flood precipitation and flooding around 142 calyr BP (Miller *et al.* 2013). At this time, the highest values of chlorite and smectite are recorded in the study core consistent with SE wind anomalies under the influence of strong tropical storms. The clay mineralogical results suggest that the potential sources of kaolinite and illite are the Sistan Basin and Jazmurian playa, while smectite is predominantly transported by aerosols and/or ocean currents from the northeastern region of the Arabian Sea. Chlorite may be transported to the sedimentary environment from both the Sistan Basin and the northeastern region of the Arabian Sea. Therefore, the sediment sources in the Gulf of Oman can be identified by plotting the clay mineral compositions on a smectite–kaolinite–illite+chlorite ternary diagram (Fig. 6).

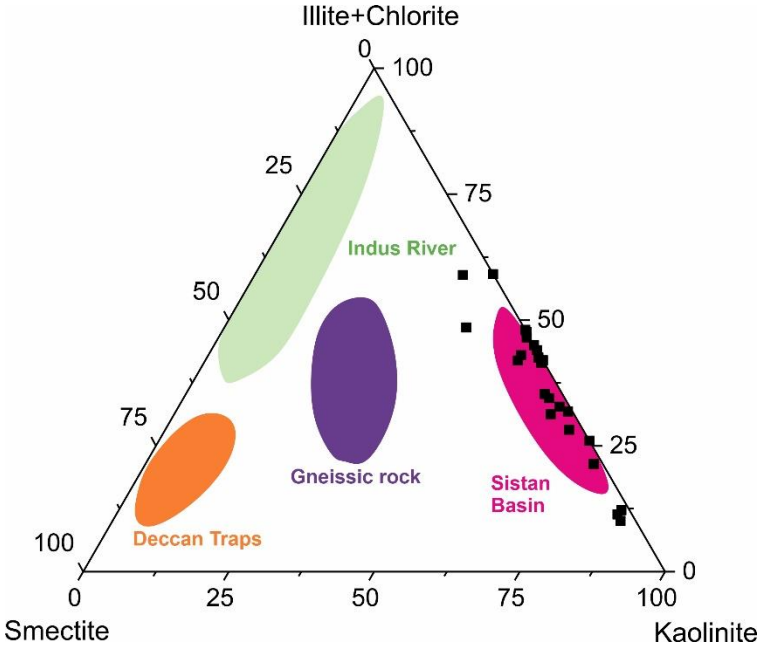

Fig. 6. Smectite–kaolinite–illite+chlorite ternary diagram showing possibility source of clay minerals in the Eastern Arabian Sea from Indus River, Deccan Traps and Gneissic rock (Rao & Rao 1995; Kessarkar *et al.* 2003; Alizai *et al.* 2012) and Gulf of Oman namely Sistan Basin.

CONCLUSION

Summer precipitation in the Arabian Sea and the Gulf of Oman have been controlled by atmospheric and oceanographic conditions. Previous studies merely focused on evidence of humid/arid climatic conditions in the marine cores. This means that the impacts of the other important parameters such as wind regimes and palaeo-environmental changes on precipitation patterns have often been overlooked. The poleward movement of the

summer monsoon is considered as a main reason for extending humid periods. In certain instances, our reconstruction shows disparities between monsoon records in Asia and the Arabian Sea.

The results of this study shed new light on precipitation sources in the Northern Arabian Sea and the Gulf of Oman and monsoon variations during the late Holocene. An elevation in the intensity of the N Levar wind and an equatorial migration of the summer monsoon belt occurred during the Roman Climatic Optimum (RCO). N Levar wind had important impacts on the basin conditions in the Gulf of Oman: (i) leading to aerosol flux to the Gulf of Oman and (ii) extending cyclonic currents in the Gulf of Oman. Cold water upwelling by Ekman pumping and increase in nutrient were created favorable condition for marine primary productivities. Decreased N Levar wind intensity led to an attenuation of Ekman transport as well as an elevation in water salinity and temperature under the influences of the Persian Gulf water outflow. Increased SST and salinity in the Northeast Arabian Sea provided the conditions for the regeneration tropical storms. Therefore, the humid climatic conditions in the Makran zone between 1900 and 1500 calyr BP were controlled by warm water accumulation to the Northeast Arabian Sea. We suggest the same trends for the warm periods.

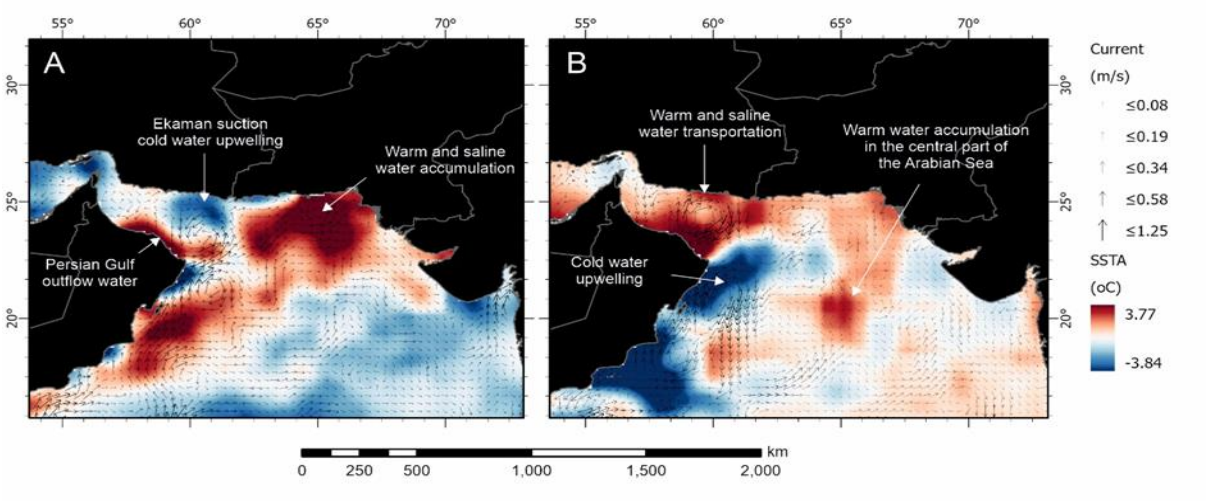

Fig. 7. Oceanographic current and Sea Surface Temperature Anomaly (SSTA) changes during post-monsoon and monsoon seasons. (A) During domination cyclonic current in the Gulf of Oman, Ekman suction effects let to upwelling warm and saline outflow water in the northern Oman coast and cold water upwelling in the northern Gulf of Oman. Accumulation of warm and saline water occurred in the northeast of the Arabian Sea. (B) domination SW summer monsoon wind led to upwelling cold water in the eastern Oman coast and transportation warm and saline water to the center of the Arabian Sea during anticyclonic current regime in the Gulf of Oman.

During the solar minimum periods, we witness a decrease in N Levar wind intensities and aerosol sources in the Sistan Basin and Jazmurian playa. Consequently, a poleward migration of the summer monsoon belt and intensification of the NW Shamal wind occurred. A solar minimum cycle during the Medieval Warm Period (MWP) led to an attenuation of the N Levar wind and a change in the geography of oceanographic currents. This period was characterized by more tropical storms and the domination of SE winds in the Northern Arabian Sea.

Since 1400 calyr BP by the domination of SW summer wind stress in the Arabian Sea, the elevated upwelling on the eastern coast of Oman, and the drop in the Persian Gulf water outflow depth, led to dominant anticyclonic currents in the Gulf of Oman, as well as the transportation of warm and saline water to the center of the Arabian Sea by oceanographic currents. By the poleward migration of the summer monsoon belt and an intensification of the NW Shamal wind, the volume of warm and saline outflow upraised, in addition to elevating in the salinity and temperature of the Gulf of Oman and in the center of the Arabian Sea. Dominant monsoon conditions in the Arabian Sea provide the required humidity and energy for tropical storms. Meanwhile, the upraise in water salinity and temperature could have significant impacts on storm strength. During late Holocene colder phases, there were two main summer precipitation sources, (i) the summer monsoon and (ii) tropical storm events.

ACKNOWLEDGEMENTS

This study was conducted as a part of the PhD dissertation of the first author (S. Amjadi) at the Ferdowsi University of Mashhad (#3/57576). This work has been mainly supported by the Centre for International Scientific Studies and Collaboration (CISSC), Ministry of Science, Research and Technology, Iran, through a research

project, number 990148. It was also partially supported by the Iranian National Institute for Oceanography and Atmospheric Science. David Kaniewski and Nick Marriner were supported by "MITI CNRS évènements rares - AQUASANMARCO program".

REFERENCES

Ahmad, I, Fenta, A, Dar, MA, Tashome, A, Halefom, A, Berhan, M & Mekuriaw, T 2022, Sources of aerosol optical depth and its distribution in Abbay basin. Ethiopia. *Applied Geomatics*, 142: 213-222.

Al Senafi, F, & Anis, A 2015, Shamals and climate variability in the Northern Arabian/Persian Gulf from 1973 to 2012. *International Journal of Climatology*, 3515: 4509-4528.

Al-Azri, AR, Piontkovski, SA, Al-Hashmi, KA, Goes, JI, & Do Gomes, HR 2010, Chlorophyll a as a measure of seasonal coupling between phytoplankton and the monsoon periods in the Gulf of Oman. *Aquatic Ecology*, 442: 449-461.

Alizadeh-Choobari, O, Zawar-Reza, P & Sturman, A 2014, The "wind of 120 days" and dust storm activity over the Sistan Basin. *Atmospheric Research*, 143: 328-341.

Alizai, A, Hillier, S, Clift, PD, Giosan, L, Hurst, A, VanLaningham, S & Macklin, M 2012, Clay mineral variations in Holocene terrestrial sediments from the Indus Basin. *Quaternary Research*, 773: 368-381.

Amjadi, S 2023, Investigation of environmental changes and reconstructions of Makran sedimentary environments using multiproxy of deep sedimentary cores of Oman Sea (SE Iran). PhD Dissertation, Ferdowsi University of Mashhad, Iran, [In Persian].

Aqrawi, AA 1993, Palygorskite in the recent fluvio-lacustrine and deltaic sediments of southern Mesopotamia. *Clay Minerals*, 281: 153-159.

Avinash, K, Kurian, PJ, Warrier, AK, Shankar, R, Vineesh, TC, & Ravindra, R 2016, Sedimentary sources and processes in the eastern Arabian Sea: insights from environmental magnetism, geochemistry and clay mineralogy. *Geoscience Frontiers*, 72: 253-264.

Azharuddin, S, Govil, P, Singh, AD, Mishra, R & Agrawal, S 2022, Mid-Holocene intensification of the oxygen minimum zone in the northeastern Arabian Sea. Journal of Asian Earth Sciences, 227: 105094.

Bailey, RW Ed 1988, *Records of Oman*: Archive Editions, 1867-1947.

Böll, A, Lückge, A, Munz, P, Forke, S, Schulz, H, Ramaswamy, V & Emeis, KC 2014, Late Holocene primary productivity and sea surface temperature variations in the northeastern Arabian Sea: Implications for winter monsoon variability. *Paleoceanography*, 298: 778-794.

Boulay, S, Colin, C, Trentesaux, A, Pluquet, F, Bertaux, J, Blamart, D & Wang, P 2003, February. Mineralogy and sedimentology of Pleistocene sediment in the South China Sea ODP Site 1144. In Proceedings of the Ocean Drilling Program, Scientific Results, 184: 1-21.

Clift, PD, Wan, S & Blusztajn, J 2014, Reconstructing chemical weathering, physical erosion and monsoon intensity since 25 Ma in the northern South China Sea: a review of competing proxies. *Earth-Science Reviews*, 130: 86-102.

Doose-Rolinski, H, Rogalla, U, Scheeder, G, Lückge, A, & von Rad, U 2001, High-resolution temperature and evaporation changes during the late Holocene in the northeastern Arabian Sea. *Paleoceanography*, 164: 358-367.

Dykoski, CA, Edwards, RL, Cheng, H, Yuan, D, Cai, Y, Zhang, M & Revenaugh, J 2005, A high-resolution, absolute-dated Holocene and deglacial Asian monsoon record from Dongge Cave, China. *Earth and Planetary Science Letters*, 2331: 71-86.

Fajemila, OT, Langer, MR, & Lipps, JH 2015, Spatial patterns in the distribution, diversity and abundance of benthic foraminifera around Moorea Society Archipelago. *French Polynesia*. PloS One, 1012: 0145752.

Fleitmann, D, Burns, SJ, Mangini, A, Mudelsee, M, Kramers, J, Villa, I & Matter, A 2007, Holocene ITCZ and Indian monsoon dynamics recorded in stalagmites from Oman and Yemen Socotra. *Quaternary Science Reviews*, 261: 170-188.

Fleitmann, D, Burns, SJ, Mudelsee, M, Neff, U, Kramers, J, Mangini, A & Matter, A 2003, Holocene forcing of the Indian monsoon recorded in a stalagmite from southern Oman. *Science*, 3005626: 1737-1739.

Forke, S, Rixen, T, Burdanowitz, N, Lückge, A, Ramaswamy, V, Munz, P & Gaye, B 2019, Sources of laminated sediments in the northeastern Arabian Sea off Pakistan and implications for sediment transport mechanisms during the late Holocene. *The Holocene*, 291: 130-144.

Garzanti, E, Vermeesch, P, Andò, S, Vezzoli, G, Valagussa, M, Allen, K, Kadi, KA & Al-Juboury, AI 2013, Provenance and recycling of Arabian desert sand. *Earth-Science Reviews*, 120: 1-19.

Ginoux, P, Prospero, JM, Gill, TE, Hsu, NC & Zhao, M 2012, Global-scale attribution of anthropogenic and natural dust sources and their emission rates based on MODIS Deep Blue aerosol products. *Reviews of Geophysics*, 503.

Golobokova, L, Khodzher, T, Khuriganova, O, Marinayte, I, Onishchuk, N, Rusanova, P & Potemkin, V 2020, Variability of chemical properties of the atmospheric aerosol above Lake Baikal during large wildfires in Siberia. *Atmosphere*, 1111: 12-30.

Govil, P, Mazumder, A, Agrawal, S, Azharuddin, S, Mishra, R, Khan, H & Verma, D 2022, Abrupt changes in the southwest monsoon during Mid-Late Holocene in the western Bay of Bengal. *Journal of Asian Earth Sciences*, 227: 105100.

Guieu, C, Al Azhar, M, Aumont, O, Mahowald, N, Lévy, M, Éthé, C & Lachkar, Z 2019, Major impact of dust deposition on the productivity of the Arabian Sea. *Geophysical Research Letters*, 4612: 6736-6744.

Hamidi, M, Kavianpour, MR & Shao, Y 2014, Numerical simulation of dust events in the Middle East. *Aeolian Research*, 13: 59-70.

Hamidi, M, Kavianpour, MR & Shao, Y 2017, A quantitative evaluation of the 3–8 July 2009 Shamal dust storm. *Aeolian Research*, 24: 133-143.

Hamzeh, MA, Gharaie, MHM, Lahijani, HAK, Djamali, M, Harami, RM & Beni, AN 2016, Holocene hydrological changes in SE Iran, a key region between Indian Summer Monsoon and Mediterranean winter precipitation zones, as revealed from a lacustrine sequence from Lake Hamoun. *Quaternary International*, 408: 25-39.

Hamzeh, MA, Khosravi, M, Carton, X, Yarahmadi, D & Safarkhani, E 2021, Paleoceanography of the Strait of Hormoz and its link to paleoclimate changes since the mid-Holocene. *Continental Shelf Research*, 226: 104507.

Hassanizade, S & Jafari, S 2021, Changes in physicochemical properties of old stabilized sand dunes due to atmospheric sediments and diversity of clay minerals in a dry area. *Aeolian Research*, 50: 100674.

Heiri, O, Lotter, AF & Lemcke, G 2001, Loss on ignition as a method for estimating organic and carbonate content in sediments: reproducibility and comparability of results. *Journal of paleolimnology*, 25: 101-110.

Holbourn, A, Henderson, AS, MacLeod, N & MacLeod, N 2013, Atlas of benthic foraminifera. *London: Wiley-Blackwell*, 654p.

Kaithwar, A, Singh, DP & Saraswat, R 2020, A highly diverse living benthic foraminiferal assemblage in the oxygen deficient zone of the southeastern Arabian Sea. *Biodiversity and Conservation*, 29: 3925-3958.

Kaskaoutis, DG, Rashki, A, Houssos, EE, Mofidi, A, Goto, D, Bartzokas, A & Legrand, M 2015, Meteorological aspects associated with dust storms in the Sistan region, Southeastern Iran. *Climate Dynamics*, 45: 407-424.

Kessarkar, PM, Rao, VP, Ahmad, SM & Babu, GA 2003, Clay minerals and Sr–Nd isotopes of the sediments along the western margin of India and their implication for sediment provenance. *Marine Geology*, 2021: 55-69.

Krivonogov, SK, Burr, GS, Kuzmin, YV, Gusskov, SA, Kurmanbaev, RK, Kenshinbay, TI & Voyakin, DA 2014, The fluctuating Aral Sea: A multidisciplinary-based history of the last two thousand years. *Gondwana Research*, 261: 284-300.

L'Hégaret, P, Lacour, L, Carton, X, Roullet, G, Baraille, R & Corréard, S 2013, A seasonal dipolar eddy near Ras Al Hamra Sea of Oman. *Ocean Dynamics*, 636: 633-659.

Ladigbolu, IA, Li, H, Li, B, Wiesner, MG, Zhang, J, Sun, L & Chen, J 2020, Calcification depths and temperatures of planktonic foraminifera off southwest Hainan Island and their paleoceanographic implications. *Marine Micropaleontology*, 158: 101878.

Lei, Y & Li, T 2016, Atlas of benthic foraminifera from China seas: The Bohai Sea and the Yellow Sea. Springer.

Li, Z, Pospelova, V, Liu, L, Francois, R, Wu, Y, Mertens, KN & Xie, X 2021, High-resolution reconstructions of Holocene sea-surface conditions from dinoflagellate cyst assemblages in the northern South China Sea. *Marine Geology*, 438: 106528.

Liao, X, Zhan, H & Du, Y 2016, Potential new production in two upwelling regions of the western Arabian Sea: Estimation and comparison. *Journal of Geophysical Research: Oceans*, 1217: 4487-4502.

Liu, Z, Colin, C, Trentesaux, A, Blamart, D, Bassinot, F, Siani, G & Sicre, MA 2004, Erosional history of the

eastern Tibetan Plateau since 190 kyr ago: clay mineralogical and geochemical investigations from the southwestern South China Sea. *Marine Geology*, 2091: 1-18.

Maghrabi, AH & Al-Dosari, AF 2016, Effects on surface meteorological parameters and radiation levels of a heavy dust storm occurred in Central Arabian Peninsula. *Atmospheric Research*, 182: 30-35.

Marriner, N & Morhange, C 2007, Geoscience of ancient Mediterranean harbors. *Earth-Science Reviews*, 803: 137-194.

Marriner, N, Morhange, C, Boudagher-Fadel, M, Bourcier, M & Carbonel, P 2005, Geoarchaeology of Tyre's ancient northern harbor, Phoenicia. *Journal of Archaeological Science*, 329: 1302-1327.

Meher-Homji, VM 1991, Probable impact of deforestation on hydrological processes. In Tropical forests and climate. *Springer, Dordrecht*, 163-173.

Miller, CS 2010, A multi-proxy palaeonenvironmental reconstruction from sediment cores, offshore Iran-Natural hazards and climatic change within the Late Holocene. *Doctoral dissertation, Brunel University Institute for the Environment MPhil Theses*.

Miller, CS, Leroy, SA, Collins, PE & Lahijani, HA 2016, Late Holocene vegetation and ocean variability in the Gulf of Oman. *Quaternary Science Reviews*, 143: 120-132.

Milliman, JD & Farnsworth, KL 2013, River discharge to the coastal ocean: a global synthesis. *Cambridge University Press*.

Modarres, R & da Silva, VDPR 2007, Rainfall trends in arid and semi-arid regions of Iran. *Journal of Arid Environments*, 702: 344-355.

Moros, M, Kuijpers, A, Snowball, I, Lassen, S, Bäckström, D, Gingele, F & McManus, JJMG 2002, Were glacial iceberg surges in the North Atlantic triggered by climatic warming? *Marine Geology*, 1924: 393-417.

Munz, PM, Siccha, M, Lückge, A, Böll, A, Kucera, M & Schulz, H 2015, Decadal-resolution record of winter monsoon intensity over the last two millennia from planktic foraminiferal assemblages in the northeastern Arabian Sea. *The Holocene*, 2511: 1756-1771.

Normand, R, Simpson, G, Herman, F, Biswas, RH & Bahroudi, A 2019, Holocene sedimentary record and coastal evolution in the Makran subduction zone Iran. *Quaternary*, 22: 1-21.

Pirrung, M, Fütterer, D, Grobe, H, Matthießen, J & Niessen, F 2002, Magnetic susceptibility and ice-rafted debris in surface sediments of the Nordic Seas: implications for Isotope Stage 3 oscillations. *Geo-Marine Letters*, 22: 1-11.

Polson, D, Bollasina, M, Hegerl, GC & Wilcox, LJ 2014, Decreased monsoon precipitation in the Northern Hemisphere due to anthropogenic aerosols. *Geophysical Research Letters*, 4116: 6023-6029.

Pourkerman, M, Marriner, N, Amjadi, S, Lak, R, Hamzeh, M, Mohammadpor, G & Shah-Hosseini, M 2023, The impacts of Persian Gulf water and ocean-atmosphere interactions on tropical cyclone intensification in the Arabian Sea. *Marine Pollution Bulletin*, 188: 114553.

Pourkerman, M, Marriner, N, Morhange, C, Djamali, M, Spada, G, Amjadi, S & Beni, AN 2020, Geoarchaeology as a tool to understand ancient navigation in the northern Persian Gulf and the harbour history of Siraf. *Journal of Archaeological Science*: Reports, 33: 102539.

Pous, SP, Carton, X & Lazure, P 2004, Hydrology and circulation in the Strait of Hormuz and the Gulf of Oman—Results from the GOGP99 Experiment: 2. Gulf of Oman. *Journal of Geophysical Research*: Oceans, 109C12.

Rao, VP & Rao, BR 1995, Provenance and distribution of clay minerals in the sediments of the western continental shelf and slope of India. *Continental Shelf Research*, 1514: 1757-1771.

Rao, VP, Shynu, R, Singh, SK, Naqvi, SWA & Kessarkar, PM 2015, Mineralogy and Sr–Nd isotopes of SPM and sediment from the Mandovi and Zuari estuaries: Influence of weathering and anthropogenic contribution. *Estuarine, Coastal and Shelf Science*, 156: 103-115.

Rashki, A, Arjmand, M & Kaskaoutis, DG 2017, Assessment of dust activity and dust-plume pathways over Jazmurian Basin, southeast Iran. *Aeolian Research*, 24: 145-160.

Rashki, A, Kaskaoutis, DG, Mofidi, A, Minvielle, F, Chiapello, I, Legrand, M, Dumka, UC & Francois, P 2019, Effects of Monsoon, Shamal and Levar winds on dust accumulation over the Arabian Sea during summer–The July 2016 case. *Aeolian Research*, 36: 27-44.

Reuter, M, Spreter, PM, Brachert, TC, Mertz-Kraus, R & Wrozyna, C 2022, Giant clam Tridacna distribution in the Gulf of Oman in relation to past and future climate. *Scientific Reports*, 121: 1-12.

Robinson, SG, Maslin, MA & McCave, IN 1995, Magnetic susceptibility variations in Upper Pleistocene deep-sea sediments of the NE Atlantic: Implications for ice rafting and paleocirculation at the last glacial maximum. *Paleoceanography*, 102: 221-250.

Saravanan, P, Gupta, AK, Zheng, H, Panigrahi, MK, Tiwari, SK, Rai, SK & Prakasam, M 2020, Response of shallow-sea benthic foraminifera to environmental changes off the coast of Goa, eastern Arabian Sea, during the last~ 6100 calyr BP. *Geological Magazine*, 1573: 497-505.

Sharifi-Yazdi, M, Tavakoli, V, Salehi-Noparvar, S, Vaezi, A, Naderi Beni, A, Nazemi, M & Routh, J 2022, Influence of the Late Quaternary climate on sedimentology of the Jazmurian Playa, SE Iran. *Journal of Paleolimnology*, 682: 169-187.

Shetye, SR, Gouveia, AD & Shenoi, SSC 1994, Circulation and water masses of the Arabian Sea. *Proceedings of the Indian Academy of Sciences-Earth and Planetary Sciences*, 103: 107-123.

Singer, A, Stahr, K & Zarei, M 1998, Characteristics and origin of sepiolite Meerschaum from Central Somalia. *Clay Minerals*, 332: 349-362.

Sinha, A, Kathayat, G, Cheng, H, Breitenbach, SF, Berkelhammer, M, Mudelsee, M & Edwards, RL 2015, Trends and oscillations in the Indian summer monsoon rainfall over the last two millennia. *Nature Communications*, 61: 6309.

Sinha, A, Kathayat, G, Weiss, H, Li, H, Cheng, H, Reuter, J & Edwards, RL 2019, Role of climate in the rise and fall of the Neo-Assyrian Empire. *Science Advances*, 511: eaax6656.

Sirocko, F, & Lange, H 1991, Clay-mineral accumulation rates in the Arabian Sea during the late Quaternary. *Marine Geology*, 971: 105-119.

Suresh, K, Kumar, A, Ramaswamy, V & Prakash Babu, C 2022, Seasonal variability in aeolian dust deposition fluxes and their mineralogical composition over the Northeastern Arabian Sea. *International Journal of Environmental Science and Technology*, 198: 7701-7714.

Thamban, M, Kawahata, H & Rao, VP 2007, Indian summer monsoon variability during the Holocene as recorded in sediments of the Arabian Sea: timing and implications. *Journal of Oceanography*, 63: 1009-1020.

Thompson, R & Clark, RM 1990, Sequence slotting for stratigraphic correlation between cores: Theory and practice. In: Paleolimnology and the Reconstruction of Ancient Environments: Paleolimnology Proceedings of the XII INQUA Congress, Springer Netherlands, pp. 229-240.

Vaezi, A, Routh, J, Djamali, M, Gurjazkaite, K, Tavakoli, V, Beni, AN & Roberts, P 2022, New multi-proxy record shows potential impacts of precipitation on the rise and ebb of Bronze Age and imperial Persian societies in southeastern Iran. *Quaternary Science Reviews*, 298: 107855.

Yadav, RK & Roxy, MK 2019, On the relationship between north India summer monsoon rainfall and east equatorial Indian Ocean warming. *Global and Planetary Change*, 179: 23-32.

Yu, C, Drake, H, Mathurin, FA & Åström, ME 2017, Cerium sequestration and accumulation in fractured crystalline bedrock: The role of Mn-Fe hydroxides and clay minerals. *Geochimica et Cosmochimica Acta*, 199: 370-389.

Yu, Y, Notaro, M, Liu, Z, Wang, F, Alkolibi, F, Fadda, E & Bakhrjy, F 2015, Climatic controls on the interannual to decadal variability in Saudi Arabian dust activity: Toward the development of a seasonal dust prediction model. *Journal of Geophysical Research: Atmospheres*, 1205: 1739-1758.

Yu, Z, Colin, C, Wan, S, Saraswat, R, Song, L, Xu, Z & Kumar, A 2019, Sea level-controlled sediment transport to the eastern Arabian Sea over the past 600 kyr: Clay minerals and SrNd isotopic evidence from IODP Site U1457. *Quaternary Science Reviews*, 205: 22-34.